Sustainable Materials and Technologies 26 (2020) e00212

Contents lists available at ScienceDirect

Sustainable Materials and Technologies

journal homepage: www.elsevier.com/locate/susmat

Spin coating method improved the performance characteristics of films obtained from poly(lactic acid) and cellulose nanocrystals

Jamileh Shojaeiarani [a,*], Dilpreet S. Bajwa [b], Nicole M. Stark [c], Teresa M. Bergholz [e], Autumn L. Kraft [d]

[a] Department of Mechanical Engineering, Western New England University, Springfield, MA 01119, United States
[b] Department of Mechanical and Industrial Engineering, Montana State University, Bozeman, MT 59717, United States
[c] USDA Forest Products Laboratory, One Gifford Pinchot Drive, Madison, WI 53705, United States
[d] Department of Microbiological Sciences, North Dakota State University, Fargo, ND 58102, United States
[e] Department of Food Science and Human Nutrition, Michigan State University, United States

ARTICLE INFO

Article history:
Received 5 June 2020
Received in revised form 27 July 2020
Accepted 15 August 2020

Keywords:
Poly(lactic acid)
Cellulose nanocrystals
Barrier properties
Antimicrobial properties
Food packaging

ABSTRACT

For the last few decades, the application of biopolymers such as poly(lactic acid, PLA) as an alternative to synthetic polymers in the packaging industry is in great demand. However, to rival the traditional polymers, the barrier properties and antimicrobial activities of PLA need to be adapted to the food packaging requirements. The purpose of this research was to compare the impact of thin-film fabrication techniques in combination with different contents of cellulose nanocrystals (CNCs) (1–5 wt%) on the barrier and antimicrobial properties of PLA films. The nanocomposite thin films were manufactured via solvent casting and spin-coating techniques. The spin-coating method has been employed for the first time in this work to prepare nanocomposite thin films with a thickness of ~ 0.2 mm. The nanocomposite films were tested for surface morphology, degree of crystallinity, water vapor permeability, contact angle, and antimicrobial properties. Scanning electron microscopy (SEM) micrographs revealed the strong tendency of CNCs to establish microscale aggregates, however, a high drying rate in the spin-coating method decreases the self-assembly in CNCs. Thus, a significantly higher degree of crystallinity and glass transition temperature were observed in spin-coated films due to a more uniform dispersion of CNCs in PLA. Higher contact angle and lower water vapor transfer rate in spin-coated samples confirmed the lower hydrophilicity character of spin-coated thin films. Two separate assays were employed for evaluating the anti-microbial activity of PLA on the foodborne pathogens. The results showed that the film manufacturing technique and CNC concentration have a strong influence on microbial reduction.

1. Introduction

Increasing concerns over climate change and human health have motivated the scientific association to improve the potential application of bio-based polymers in diverse fields. Food packaging industry represents an important sector with consumption of different petroleum-based materials with short term applications [1]. In this regards, bio-based and bio-degradable polymers with high potential of decreasing the dependency on conventional plastic have been extensively explored during recent decades [7,40]. The primary goal of food packaging is protecting foods from damages caused by pathogens, moisture, light, and heat, etc. The right selection of food packaging materials can prolong the shelf life of a food product [24]. The spoilage of food due to microbial metabolism alternations and foodborne pathogens is considered as one of the utmost losses in food industry, and packaging materials can control the food quality to some extent [6]. The protective packaging films can control the microbial activity in food products by creating an active barrier, expanding the lag time, and decreasing the microorganisms' growth in food products.

Polylactic acid (PLA), the most commonly used biopolymer in food packaging sector, accounts for compound annual growth rate (CAGR) of 19.5% and is estimated to achieve a market of $6.5 billion by 2025 [35]. PLA is being explored as a promising substitution for petroleum-based polymers in the packaging industry, owing to its biodegradability, biocompatibility, and sustainability. The biocompatible nature of PLA makes it an ideal choice as packaging material with a wide spectrum of food packaging applications. The general physical properties, melt processing simplicity and easy of processability of PLA are comparable to petroleum-based packaging resins [33].

Generally, a polymer is acceptable in the food packaging industry when it can fulfill the required optimal characteristics of food products [34]. Barrier property is an important characteristic in polymer materials which may impact their suitability for a specific application and

* Corresponding author.
E-mail addresses: jamileh.shojaeiarani@wne.edu (J. Shojaeiarani), dilpreet.bajwa@montana.edu (D.S. Bajwa), nstark@fs.fed.us (N.M. Stark), tmb@msu.edu (T.M. Bergholz), autumn.l.kraft@ndsu.edu (A.L. Kraft).

https://doi.org/10.1016/j.susmat.2020.e00212
2214-9937/

generally, it is a function of the degree of crystallinity, crystalline/amorphous phase ratio, structural properties, and the polarity of the polymeric chains [23,25].

Compared to synthetic polymers PLA exhibits similar impermeability to carbon dioxide (CO_2) and oxygen (O_2), however, it has relatively high permeability to small molecules including water vapor (WV), and organic vapors molecules [23]. The poor barrier properties in PLA as compared with selected petroleum-based polymers impose restrictions over its commercial application in the packaging industry. To advance the mechanical, barrier and thermal behavior of PLA, different nano-sized fillers such as cellulose and lignin [41], graphene [27], zinc oxide [30] nanoparticles have been added into the polymer matrix. In addition to barrier properties of PLA thin film, its antimicrobial effect of PLA against selected microorganisms has been studied through incorporating different natural antimicrobial agents such as lysozyme [8], chitosan powder [39], and limonene [29].

Among different nanofillers, cellulose nanocrystals (CNCs), an emerging class of nature-derived nanoparticles, have received noticeable attention over the past few decades owing to their lightweight character (density ca. 1.56 g cm^{-3}), high aspect ratio (approximately 70), large surface area (around 150 m^2/g), and highly crystalline structure. It was reported that incorporating CNCs into PLA can improve the barrier properties of PLA, and serve as potential option for storing different types of food products [9,10,17,21]. The improvement is ascribed to the arrangement of a rigid hydrogen-bonded network controlled by a percolation mechanism [4]. The gases permeability through nanocomposites thin films is governed by various features such as tortuosity of gaseous molecules path through the nanocomposite structure, nanofiller type, aspect ratio, and content, degree of dispersion, and interfacial interaction between nanofillers and matrix [28]. In the application of CNCs as nanofillers in PLA matrix, a uniform dispersion is required to benefit the optimized barrier influence of CNCs in nanocomposite film. Poor CNCs' dispersion considerably restricts the enhancement in the barrier properties of the nanocomposite thin films.

Most of the researches reported in the literature used solvent casting technique for thin-film fabrication and there is a need for a new technique in enhancing the dispersion of CNC in PLA matrix using different methods. The spin-coating method is a simple and quick thin film preparation method. It can offer ultrathin polymer film with even thickness. The presence of centrifugal driving force as well as surface tension in the spin-coating method can result in uniform dispersion of nanofillers in the matrix and thin-film with a desirable thickness (Fig. 1) [15,19].

In this research, nanocomposite thin films were manufactured via solvent casting and spin-coating methods. While, solvent casting is a common thin film making technique, spin-coating method has been used for the first time in this work to prepare nanocomposite thin films. The effect of two manufacturing techniques in combination with CNCs loading on the barrier and antimicrobial behavior of PLA-CNCs nanocomposite films were investigated through light transmission, crystallization, and antimicrobial analysis.

2. Experimental

2.1. Materials

Poly(lactic acid) (PLA 2002D, $M_n = 98{,}000\ gmol^{-1}$) was purchased from NatureWorks LLC (Minnetonka, MN, USA). Wood-based cellulose nanocrystals with a dimensions of 150 nm length and 7 nm width were kindly supplied by USDA-Forest Service (Forest Products Lab., Madison, WI, USA). Analytical grade chloroform used in this research was purchased from Sigma-Aldrich (St. Louis, MO, USA).

2.2. Film preparation

To compare the effect of manufacturing methods on nanocomposite thin films barrier properties, PLA-based nanocomposite thin films were manufactured via two different methods, including solvent casting and spin-coating methods. For each formulation, PLA solution was prepared by dissolving 7 g PLA pellets in 70 ml chloroform under magnetic stirring at room temperature (~24 °C) until all pellets were disappeared. Direct dispersion of CNCs into chloroform have reported challenges of agglomeration; in this study to overcome the challenge of nonuniform dispersion, CNCs suspension was prepared separately by dispersing CNCs in the chloroform using vigorous magnet stirring for 2 h at room temperature, followed by homogenizer (IKA Works, Wilmington, NC, USA) for 5 min, and sonication (Misonix sonicator 3000, Vernon Hills, IL, USA) for 3 min in an ice bath. The predetermined amount of CNCs suspension was then added to the PLA solution to prepare PLA-CNCs mixture with 1, 3, and 5 wt% CNCs and then exposed to vigorous stirring for 3 h. In the solvent casting method, the PLA-CNC mixture was poured into a glass Petri dishes and dried at ambient temperature for approximately 30 h. In the spin-coating method, a vacuumed spin-coater (WS-400-6NPP-Lite, Laurell Technologies, PA, USA) was used to prepare thin film nanocomposites with an even thickness. The PLA-CNCs mixture was injected into the center of the spinning substrate and the spinning step was kept constant for 180 s at 150 rpm. Then the solvent was evaporated at room temperature for 4 h and the films were solidified.

The thickness of thin films strongly influences the water vapor permeability in food packaging products. It was shown that water vapor permeability increases as the film thickness increases [5,34]. So, the thickness of thin films was kept constant in the range of 0.17–0.2 mm for all formulations. Thickness of the nanocomposite films were measured at five different points with an electronic micrometer (Mitutoyo 293–340-30, Shiwa, Japan) and the average value was reported as thickness of the film. The nanocomposite thin films of different formulations are shown in Table 1.

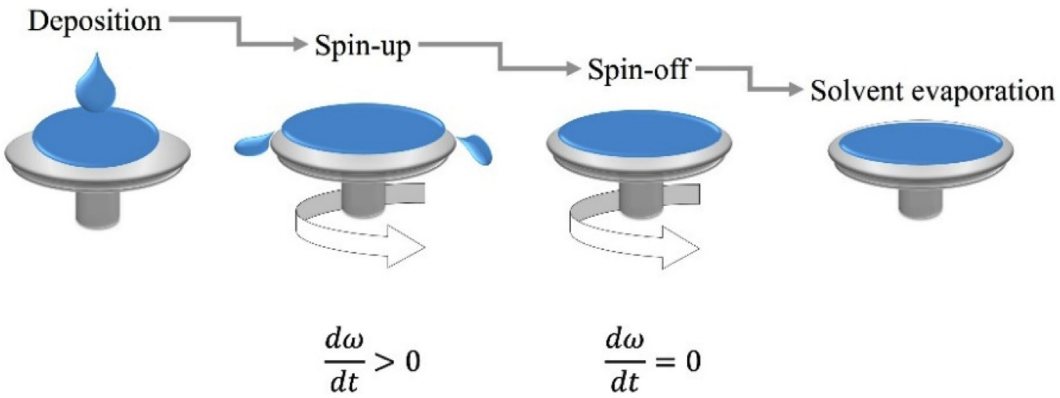

Fig. 1. Schematic diagram of thin film formation in spin-coating method.

Table 1
The compositions detail of nanocomposite films prepared via solvent casting (so) and spin-coating methods (sp).

Formulation code	PLA (wt%)	CNCs (wt%)	Film making technique
PLA-1CNC-so	99	1	Solvent casting
PLA-3CNC-so	97	3	Solvent casting
PLA-5CNC-so	95	5	Solvent casting
PLA-1CNC-sp	99	1	Spin-coating
PLA-3CNC-sp	97	3	Spin-coating
PLA-5CNC-sp	95	5	Spin-coating

2.3. Scanning Electron microscopy (SEM)

The surface morphology of thin films was characterized using a scanning electron microscope (SEM, JSM-6010LA, JEOL Inc., Peabody, MA, USA). Samples with an approximate area of 4 mm^2 were mounted on stubs with double-sided conductive tape and sputter-coated with gold to prevent electrical charging. SEM images were taken with an electron beam energy of 20 kV at a magnification of 500 × .

2.4. Differential scanning calorimetry (DSC)

It is well established that high crystallinity implies low permeability and high barrier properties in polymer film. Therefore, the non-isothermal crystallization and melting behavior of samples were evaluated using differential scanning calorimeter (TA Instrument, Q200, New Castle, DE, USA). In this regard, samples were heated from 25 to 200 °C at a heating rate of 5 °C/min under nitrogen atmosphere (the flow rate of 50 ml/min). Three such measurements were taken on each formulation and average values of thermal characteristics and crystallization behavior are reported. The degree of crystallinity of all samples was calculated using melting heat (ΔH_m), and the heat of crystallization (ΔH_C) (Eq. (1)).

$$x\% = \frac{\Delta H_m - \Delta H_c}{\Delta H_m^{100\%}} \times 100 \quad (1)$$

in which, $\Delta H_m^{100\%}$ is melting enthalpy for a 100% crystalline PLA sample, taken as 93.16 j/g [37].

2.5. Water vapor transfer rate (WVTR)

The water vapor transmission rate in nanocomposite films was measured gravimetrically, following the desiccant method in ASTM E96 with 68–3000 EZ-Cup vapometer assemblies (Thwing-Albert Instrument Company, West Berlin, NJ, USA). Samples were measured in five locations for thickness consistency and the average values were used. Nanocomposite films were conditioned at 21 °C and 50% relative humidity for 14 days prior to conducting the water vapor transmission test, and all testing was performed at 21 °C and 50% relative humidity. Desiccant (anhydrous calcium chloride) was placed in the base of the cup within 6 mm of the specimen. Film samples were cut into circles with a radius of 6.35 cm, sandwiched between two neoprene gaskets, and placed in the cup. An aluminum threated ring and Teflon seal secured the sample. The assembles were weighed periodically to establish the linear region for the curve of weight gain as a function of time. The water vapor permeability rate (WVPR) was calculated using Eq. (2):

$$WVTR = \frac{G}{t \times A} \quad (2)$$

where G/t is the weight loss per unit time (g/h) and can be obtained from the slope of the fitted straight line and A represents the area exposed to moisture transfer (m^2) (31.66 cm^2).

The film water vapor permeability (WVP) was calculated following Eq. (3):

$$WVP = \frac{WVTR}{(R_1 - R_2) \times S} \times t \quad (3)$$

in which S represents saturation vapor pressure of water at the test temperature (2493 Pa), R_1 is the fractional RH on the vapor source side (50%), R_2 denotes the fractional RH on the sink side (0%), and t is the film thickness.

2.6. Contact angle

The hydrophilicity of nanocomposite films was studied based on the measurement of water contact angles, using a video contact angle measurement system (FTA1000 B Class by First Ten Angstroms, Inc.). A droplet of water with an approximate volume of 4 μL was dropped on the surface of thin films. A high-speed digital video camera operating at 250 frames per second and accompanying software of the instrument was used to monitor the shape and edge profile of droplets in contact with the film.

2.7. Antimicrobial properties

For thin film diffusion and direct inoculation assay three different strains including RIMD 0509952 Enterohemorrhagic *Escherichia coli* (EHEC) O157:H7, ATCC BAA-1045 *Salmonella enterica* Enteritidis, and *Listeria monocytogenes* strain 10403S were used. Each strain was prepared from a − 80 °C 10% glycerin stock and streaked for isolation on either Luria-Bertani agar (LB, EHEC and *S. enterica*) or Brain Heart Infusion agar (BHI, *L. monocytogenes*). The plates were incubated at 37 °C overnight and isolated colonies were picked for inoculation of 5 ml LB broth (EHEC, *S. enterica*) or BHI broth (*L. monocytogenes*). Broth cultures were incubated with shaking at 37 °C, 215 rpm, for 16 h. After incubation, cells were prepared differently for each assay. For the thin-film diffusion assay, the culture was directly used to inoculate the LB and BHI plates. To conduct the direct inoculation assay, cells were pelleted via centrifugation (Avanti J-25 Centrifuge, Beckman Coulter, Brea, CA), growth media was removed, and resuspension of cells was done with 500 ml of phosphate-buffered saline (PBS) to concentrate the inoculum. The starting concentration of the inoculum on the disk was verified by plate count to be 10^8 colony forming units per ml (CFU/ml).

2.8. Thin film diffusion assay

Thin film used in the assay were prepared as described and sterilized by dipping into 100% ethanol and allowing to air dry before use. Using the prepared inoculum, a confluent lawn of bacteria was streaked on appropriate growth media using sterile swabs. Along with a plate used for the assay, a confluently streaked plate for each strain was prepared without thin-film disks for later comparison. Immediately after streaking, sterilized disks were placed in designated quadrants of the agar via sterile forceps and plates were incubated at 37 ^{0}C over night. Images were taken of each plate using the Q-Count (Model 530, Spiral Biotech) and zones of inhibition around the disks were measured in mm. Each culture was individually prepared three times and subjected to the disk diffusion assay with three replicates of each disk type.

The direct inoculation assay was conducted in 6-well plates, with three replicates of each pathogen and three replicates of each disk with 9 mm dimeter and 0.17–0.2 mm thickness. The prepared concentrated inoculum was placed directly onto ethanol-sterilized disks with 10: l of each culture placed on the disk surface. Disk surfaces were dried in the biosafety cabinet before the 24 h incubation period at room temperature. After the 24 h incubation, disks were removed using sterile forceps and retained in a 50 ml centrifuge tube containing 10 ml sterile PBS and acid-washed glass beads. These tubes were vortexed for 2 min and samples were diluted and plated on appropriate

growth media. Plates were incubated at 37 °C over night and colonies were enumerated using the Q-Count.

3. Results and discussion

3.1. Scanning Electron microscopy (SEM)

The surface morphology and topographies of the PLA-CNCs thin films was studied using SEM images (Fig. 2). The presence of CNC aggregates in the spherical shape for all samples indicates the strong interactions between unmodified CNCs to form bundles in the PLA matrix. Moreover, the SEM images revealed that the increase in the concentration of CNCs resulted in relatively bigger CNCs aggregates in each set of samples. The tendency to agglomerate in CNCs can be attributed to the drying conditions during preparing of the thin film. Unlike the solvent cast samples, the smaller size and more homogeneous distribution of the CNCs was observed in the spin-coated films, particularly with low CNC contents (1 and 3%). The key parameters in resisting the formation of micro-sized agglomerates in spin-coated films were high solvent evaporation rate, and the combination of centrifugal force and surface tension during the spin-coating process (Fig. 1). This hypothesis can be supported by CNC aggregates occurrence in spray-dried CNC at higher liquid feed due to the long drying process. Large chunks of CNC aggregates with sizes as high as 5–10 μm were visible throughout the film prepared through the solvent casting technique. In fact, longer drying time in the solvent cast method provides enough time for CNCs to self-assemble and form aggregates.

3.2. Differential scanning calorimetry (DSC)

Crystallinity is an important feature in polymers and governs the biodegradation rate of biodegradable polymers. In this research, the crystallization behavior of PLA-CNC nanocomposite thin films prepared through two different methods (solvent casting and spin-coating) were studied using differential scanning calorimeter (DSC) and the representative curves of DSC are shown in Fig. 3. In case of thin-film nanocomposites, there are different factors affecting the glass transition temperature, including density, interface interaction, and confinement effect. The DSC results showed that the crystallinity and thermal behavior of nanocomposite films were marginally influenced by film making methods. The glass transition temperature (T_g), taken at the mid-point of heat capacity changes was slightly higher in spin-coated samples in comparison with solvent cast films. The higher crosslinking degree promoted by uniform CNC dispersion in PLA matrix in spin-coated samples produced interactions strong enough to slow down the polymer chain mobility [31,32]. As expected, PLA-1CNC-sp with uniform CNCs dispersion (Fig. 2d) exhibited the highest value of T_g, followed by PLA-1CNC-so. In all nanocomposite samples, a noticeable reduction in T_g was observed with an increase in CNCs loading, which was more evident in solvent cast thin films. In agreement with previous study [22], the overloading of CNCs led to the formation of micro-sized agglomerates in polymer matrix, inhibiting the rotational backbone motions of PLA polymer chain and restricting increase in T_g.

In the case of crystallization temperature (T_c), an evident shift to higher values was detected for all nanocomposite thin films with respect to PLA thin film, showing that CNCs performed as heterogeneous nucleating agents in PLA matrix [11].

The crystallization temperatures for spin-coated thin film reinforced with 1, 3, and 5% CNCs were about 4, 6, and 7 °C higher than those for the solvent cast films. The relatively higher T_c in spin-coated samples in comparison with solvent cast films clearly demonstrates that more uniformly distributed CNCs in PLA matrix were able to promote the cold crystallization of PLA matrix (Fig. 2) [36]. Meanwhile, in each set of nanocomposite thin films with the addition of CNCs a slight decrement in the crystallization-temperature was observed due to the formation of micro-sized CNC aggregates through polymer matrix. Regardless of composition and film making techniques, T_m of PLA-CNC nanocomposites remains roughly constant when cellulose nanocrystals are added.

The degree of crystallinity as a long-range order in semi-crystalline polymers has a strong effect on barrier properties. The degree of crystallinity in spin-coated nanocomposites reinforced with 1, 3, and 5% CNCs was 52%, 47%, and 19% higher than that in solvent cast films with the same CNC contents. The higher degree of crystallinity in spin-coated films can be related to more uniform CNCs dispersion through PLA as shown in Fig. 2b [2]. The high solvent evaporation rate in spin-coating method improved the molecular order, and the presence of residual solvent in spin-coated samples effectively improved self-organization in polymer chain in forming a highly crystalline structure [26]. More uniform dispersion of CNCs in spin-coated films resulted in the formation of the network-like structure of CNCs in the PLA matrix, and this, in

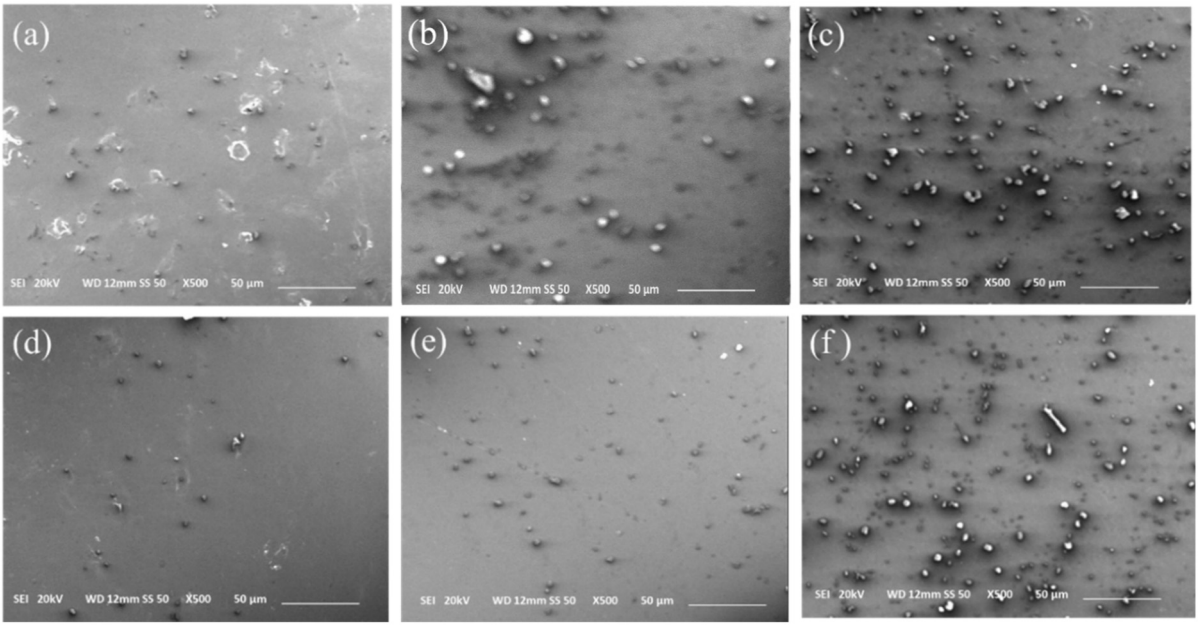

Fig. 2. Scanning electron microscopy micrographs of thin films a) PLA-1CNC-so, b) PLA-3CNC-so, c) PLA-5CNC-so, d) PLA-1CNC-sp, e) PLA-3CNC-sp and f) PLA-5CNC-sp.

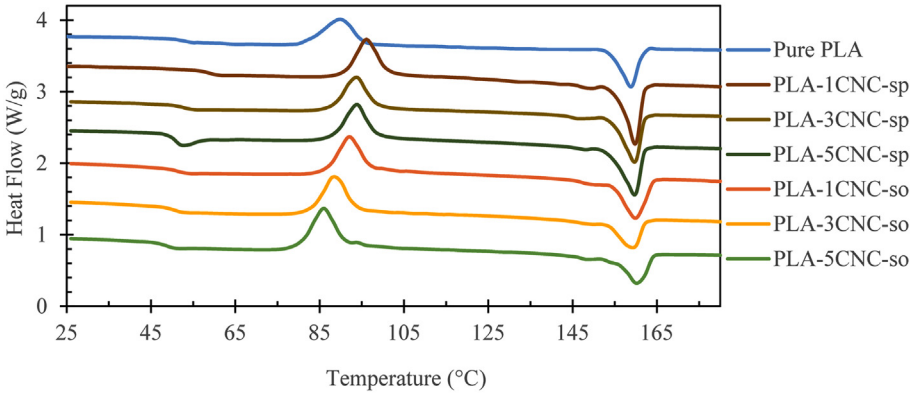

Fig. 3. Representative DSC curves of nanocomposite thin films.

turn, resulted in a higher nucleation agent effect [2,13,38]. Besides, the broad endotherm shape in solvent cast thin films indicated the high heterogeneity and different degree of perfection in solvent cast thin film nanocomposites. Although the variation of CNCs loading played the key role in thermal behavior of thin films (T_g, T_c), thin film preparation techniques had the predominant impact on degree of crystallinity. It is more likely due to heterogeneous dispersion of CNCs in spin-coated thin films (Fig. 2).

3.3. Water vapor transfer rate (WVTR)

The barrier properties of thin films are crucial for a specific application in different fields such as food packaging. In this study gravimetric Intelligent Gravimetric Analyzer (IGA)- system was employed for an accurate and fast measurement of water vapor permeability in nanocomposite films and the results are summarized in Table 3. From WVTR results it can be observed that the film preparation technique marginally affected the water vapor transfer rate. The water vapor permeability for each set of samples was close to one another. However, the water vapor permeability (WVP) values in spin-coated thin films were slightly lower than those observed in solvent cast nanocomposite thin films. This observation can be explained by the interaction between CNCs and PLA matrix in spin-coated thin films. In agreement with [20], the tortuous path in the polymer matrix reinforced by CNCs via spin-coating method was a result of uniform dispersion of CNC in PLA matrix, improved crystallinity [18], and interfacial interactions between CNCs and PLA (Fig. 2).

3.4. Contact angle

Wettability of solid film characterized based on the surface topography and hydrophilicity is classified into several levels. For the surface with a contact angle lower than 90°, the liquid will wet the contact surface and spread over it, while the contact angle higher than 90° represents hydrophilic materials. The contact angle depends on several factors, including surface roughness, topography, and the method of film preparation [12]. The features of the edge profiles of a water drop on nanocomposite films are given in Table 3 and it can be observed that by increasing the concentration of CNC, both solvent cast and spin-coated samples exhibited higher hydrophilicity character, probably due to the mediocre dispersion of CNC at higher amount (Fig. 2). While comparing the two preparation methods, the higher contact angle was observed for spin-coated films, signifying lower hydrophilicity character in spin-coated thin films. This observation was more likely due to a higher degree of crystallinity in spin-coated films as detected in Table 2 [16]. Spin-coated thin films reinforced by 1, and 3% CNCs still displayed hydrophobic surfaces with contact angle higher than 65°, showing enough hydrophobicity for different applications, such as food packaging and filtration membranes [14]. However, solvent cast thin films exhibited contact angle lower than 65° in all formulations (PLA-1CNC-so, PLA-3CNC-so, PLA-5CNC-so). It seems that in the case of contact angle and surface wettability, both different manufacturing method, and compositions led to different hydrophilicity character in nanocomposite thin films, however, the effect of manufacturing method was more predominant. The typical contact angle in the solvent cast and spin-coated thin films reinforced with CNCs are illustrated in Fig. 4.

Table 2
Thermal characteristics of nanocomposite thin films.

Formulation code	T_g (°C)	T_c (°C)	T_m (°C)	X%
Pure PLA	53.2 ± 0.3	90.6 ± 0.2	159.7 ± 0.4	1.9 ± 0.0
PLA-1CNC-so	56.7 ± 0.4	92.5 ± 0.4	160.1 ± 0.6	2.7 ± 0.1
PLA-3CNC-so	51.5 ± 0.3	88.9 ± 0.6	159.7 ± 0.7	2.3 ± 0.2
PLA-5CNC-so	50.7 ± 0.5	86.4 ± 0.3	160.0 ± 0.5	2.1 ± 0.1
PLA-1CNC-sp	57.6 ± 0.5	96.5 ± 0.5	159.5 ± 0.7	4.1 ± 0.2
PLA-3CNC-sp	52.5 ± 0.3	94.3 ± 0.7	160.3 ± 0.8	3.4 ± 0.1
PLA-5CNC-sp	52.1 ± 0.6	93.6 ± 0.2	159.8 ± 0.6	2.5 ± 0.1

3.5. Antimicrobial properties

Two separate assays were employed to evaluate the antimicrobial activity of PLA-CNC films on the foodborne pathogens *Salmonella enterica*, enterohemorrhagic *Escherichia coli* (EHEC), and *Listeria monocytogenes*. First, a disk diffusion method was used. This is a standard method of measuring the effects of antimicrobial agents on bacteria. For the assay conducted with these PLA films, no growth inhibition was observed in the bacterial lawn around the disks (data not shown). This could be due to factors such as the diffusibility of the PLA-CNC.

In a separate approach, the three tested pathogens were directly inoculated onto the nanocomposite films, incubated for 24 h, and viable cells were collected from the disks by washing with PBS and glass beads. The bacterial counts collected after the 24 h incubation was compared to the initial concentrations and the differences in the average change in log CFU/ml were calculated (Fig. 5). It was observed that these nanocomposite films affected these tested organisms differently. Of note, the L. *monocytogenes* was negatively impacted by the films during incubation with decreases reaching 0.5–0.6 log CFU/ml. *S. enterica* appeared to have no change in log CFU/ml over the 24 h incubation on any of the tested films, while EHEC had a small negative effect observed (0.1–0.2 log decrease). These differences reflect previous work done with PLA-CNC films, which had also been combined with oregano essential oil (oregano EO) and reduced graphine oxide (rGO) (Salmieri et al., 2014). In these studies, results showed that the addition of the third component negatively impacted the survival of L. *monocytogenes* (oregano EO) and *E. coli* (rGO) significantly when compared to PLA-CNC alone. Still, there appeared to be some antimicrobial effect of just PLA-

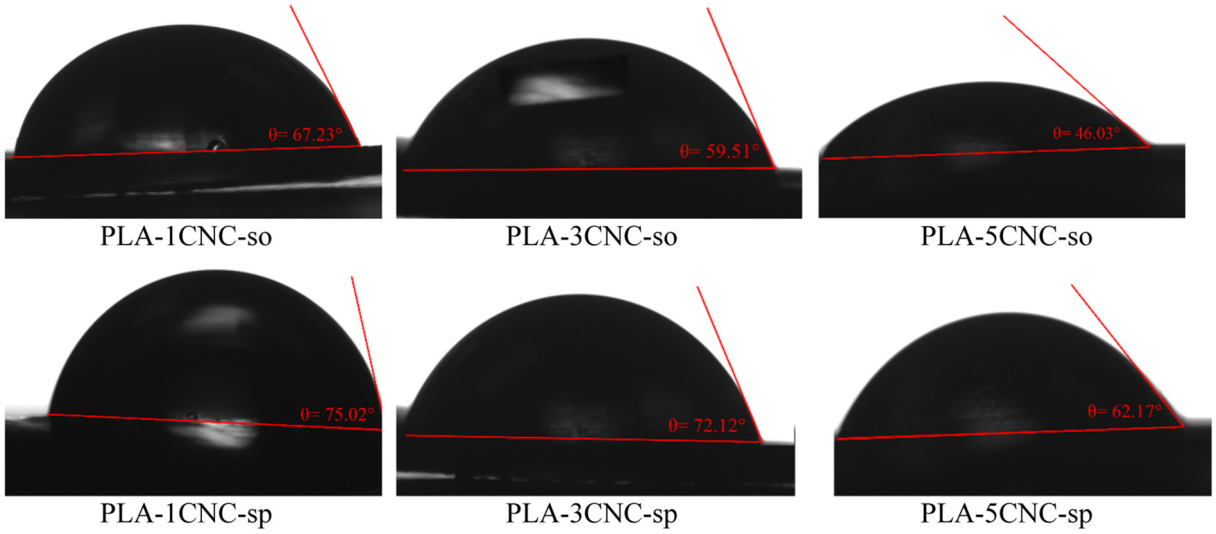

Fig. 4. Representative contact angle measurements on spin-coated and solvent cast thin films reinforced by CNCs.

Table 3
Water vapor permeability of thin PLA films reinforced with 1, 3, and 5% CNCs prepared via two different techniques: solvent casting (So) and spin-coating method (Sp).

Formulation code	WVTR (g/h/m^2)	Thickness (mm)	WVP (g/s/m/Pa) ($\times 10^{-11}$)	Contact angle
Pure PLA	0.32 ± 0.04	0.193	1.87 ± 0.11	60.08 ± 0.65
PLA-1CNC-so	0.53 ± 0.01	0.199	2.42 ± 0.02	64.01 ± 0.98
PLA-3CNC-so	0.55 ± 0.01	0.196	2.50 ± 0.11	61.70 ± 1.51
PLA-5CNC-so	0.57 ± 0.02	0.172	2.65 ± 0.02	46.68 ± 1.71
PLA-1CNC-sp	0.49 ± 0.02	0.186	2.11 ± 0.06	75.96 ± 1.36
PLA-3CNC-sp	0.51 ± 0.02	0.178	2.12 ± 0.16	73.66 ± 1.22
PLA-5CNC-sp	0.52 ± 0.02	0.183	2.20 ± 0.02	62.72 ± 0.40

CNC film on L. *monocytogenes* survival with a ~ 0.5 log reduction after two weeks when compared to no treatment (Salamari et al., 2014), a result that is similar to the reduction seen in this study. The work was done by Pal, et al. displayed that the gram-negative *E. coli* was less impacted by rGO than the gram-positive *Staphylococcus aureus*. These data reflect the distinct differences between the survival of L. *monocygtogenes* (gram-positive) and the gram-negatives *E. coli* and *S. enterica* observed after the 24 h incubation (Fig. 5). The CNC concentration led to greater reduction in L. *monocytogenes* numbers when compared to the PLA only control.

4. Conclusion

Concerns on food safety, environment, and limitations of the world's oil sources have promoted the development of antibacterial packaging materials with superior barrier properties from biobased polymers such as poly(lactic acid, PLA). In this regard, thin-film from PLA reinforced with cellulose nanocrystals (CNCs) with contents ranging from 1 to 5 wt% were prepared using solvent casting and spin-coating methods. The SEM results indicated solvent cast films exhibited poor CNCs dispersion and lower transparency in comparison with spin-

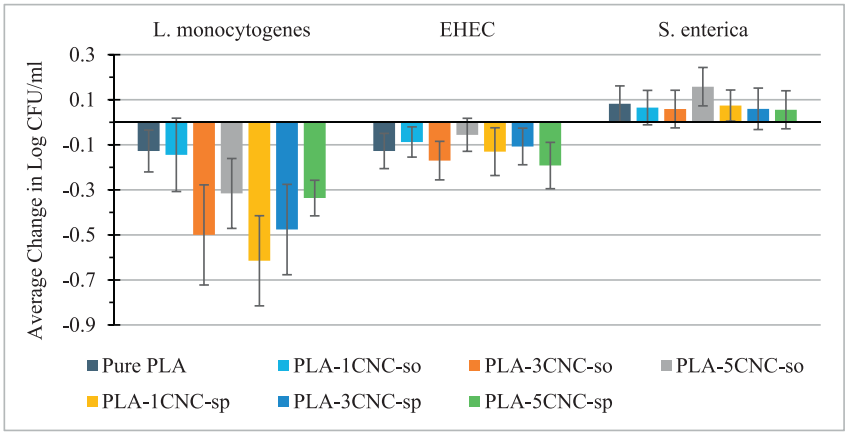

Fig. 5. Average change in Log CFU/ml of the *Listeria monocytogenes*, Enterohemorrhagic *Escherichia coli* (EHEC), and *Salmonella enterica* strains after 24 h incubation on seven different PLA film configurations (pure PLA; So or Sp; 1, 3, or 5% CNCs).

coated films. This observation was more likely due to the high drying rate in spin-coating method which limits the self-assembly of nanoparticles in polymer matrix. Moreover, the well-dispersed CNCs in the spin-coated films acted as nucleating agents, accelerating the crystallization process, and enhancing the degree of crystallinity in spin-coated films. The higher contact angle and lower water vapor permeability confirmed the lower hydrophilicity character in spin-coated films reinforced with a low concentration of CNCs (i.e. 1 and 3%). Overall, the role of centrifugal force in combination with surface tension in spin-coating manufacturing process improved the dispersion of CNCs in PLA matrix, and this, in turn resulted in improvement in degree of crystallinity, contact angle, and crystallization temperature. On the other hand, the manufacturing process exhibited more predominant effect on aforementioned characteristics than CNC loadings. The antimicrobial test of nanocomposite films against foodborne pathogens exhibited the nanocomposite films obtained from different manufacturing techniques that affected these foodborne pathogens differently.

Author statement

Jamileh Shojaeiarani, carried out the experiments, analyzed the results and wrote the manuscript. Nicole M. Stark conducted Water Vapor Transfer test. Teresa M. Bergholzd, and Autumn L. Kraft conducted Antimicrobial test. Dilpreet S. Bajwa designed the experiments and reviewed findings of this work.

Declaration of Competing Interest

The authors declare that they have no known competing financial interests or personal relationships that could have appeared to influence the work reported in this paper.

Acknowledgement

Funding for the present work was provided by National Science Foundation, NSF EPSCoR – INSPIRE-ND 1355466.

References

[1] A.L. Andrady, Plastics and the Environment, John Wiley & Sons, 2003.
[2] M.P. Arrieta, E. Fortunati, F. Dominici, E. Rayón, J. López, J.M. Kenny, Multifunctional PLA–PHB/cellulose nanocrystal films: processing, structural and thermal properties, Carbohydr. Polym. 107 (2014) 16–24.
[4] M.A.S. Azizi Samir, F. Alloin, A. Dufresne, Review of recent research into cellulosic whiskers, their properties, and their application in nanocomposite field, Biomacromolecules 6 (2) (2005) 612–626.
[5] N. Benbettaïeb, M. Kurek, S. Bornaz, F. Debeaufort, Barrier, structural and mechanical properties of bovine gelatin–chitosan blend films related to biopolymer interactions, J. Sci. Food Agric. 94 (12) (2014) 2409–2419.
[6] M.C. Biswas, B.J. Tiimob, W. Abdela, S. Jeelani, V.K. Rangari, Nano silica-carbon-silver ternary hybrid induced antimicrobial composite films for food packaging application, Food Packag. Shelf Life 19 (2019) 104–113.
[7] P. Bordes, E. Pollet, L. Avérous, Nano-biocomposites: biodegradable polyester/nanoclay systems, Prog. Polym. Sci. 34 (2) (2009) 125–155.
[8] V. Bugatti, A. Sorrentino, G. Gorrasi, Encapsulation of lysozyme into halloysite nanotubes and dispersion in PLA: structural and physical properties and controlled release analysis, Eur. Polym. J. 93 (2017) 495–506.
[9] P. Dhar, S.S. Gaur, N. Soundararajan, A. Gupta, S.M. Bhasney, M. Milli, A. Kumar, V. Katiyar, Reactive extrusion of polylactic acid/cellulose nanocrystal films for food packaging applications: influence of filler type on thermomechanical, rheological, and barrier properties, Ind. Eng. Chem. Res. 56 (16) (2017) 4718–4735.
[10] E. Fortunati, M. Peltzer, I. Armentano, L. Torre, A. Jiménez, J.M. Kenny, Effects of modified cellulose nanocrystals on the barrier and migration properties of PLA nano-biocomposites, Carbohydr. Polym. 90 (2) (2012) 948–956.
[11] E. Fortunati, D. Puglia, F. Luzi, C. Santulli, J.M. Kenny, L. Torre, Binary PVA bio-nanocomposites containing cellulose nanocrystals extracted from different natural sources: part I, Carbohydr. Polym. 97 (2) (2013) 825–836.
[12] K. Grundke, K. Pöschel, A. Synytska, R. Frenzel, A. Drechsler, M. Nitschke, A.L. Cordeiro, P. Uhlmann, P.B. Welzel, Experimental studies of contact angle hysteresis phenomena on polymer surfaces—toward the understanding and control of wettability for different applications, Adv. Colloid Interf. Sci. 222 (2015) 350–376.
[13] A. Gupta, W. Simmons, G.T. Schueneman, D. Hylton, E.A. Mintz, Rheological and thermo-mechanical properties of poly (lactic acid)/lignin-coated cellulose nanocrystal composites, ACS Sustain. Chem. Eng. 5 (2) (2017) 1711–1720.
[14] A. Hambleton, M.-J. Fabra, F. Debeaufort, C. Dury-Brun, A. Voilley, Interface and aroma barrier properties of iota-carrageenan emulsion–based films used for encapsulation of active food compounds, J. Food Eng. 93 (1) (2009) 80–88.
[15] Y.-K. Hong, H. Kim, G. Lee, W. Kim, J.-I. Park, J. Cheon, J.-Y. Koo, Controlled two-dimensional distribution of nanoparticles by spin-coating method, Appl. Phys. Lett. 80 (5) (2002) 844–846.
[16] N.K. Kalita, M.K. Nagar, C. Mudenur, A. Kalamdhad, V. Katiyar, Biodegradation of modified poly (lactic acid) based biocomposite films under thermophilic composting conditions, Polym. Test. 76 (2019) 522–536.
[17] H. Kargarzadeh, M. Mariano, J. Huang, N. Lin, I. Ahmad, A. Dufresne, S. Thomas, Recent developments on nanocellulose reinforced polymer nanocomposites: a review, Polymer 132 (2017) 368–393.
[18] S.S. Karkhanis, N.M. Stark, R.C. Sabo, L.M. Matuana, Water vapor and oxygen barrier properties of extrusion-blown poly (lactic acid)/cellulose nanocrystals nanocomposite films, Compos. A: Appl. Sci. Manuf. 114 (2018) 204–211.
[19] E. Kontturi, L.-S. Johansson, K.S. Kontturi, P. Ahonen, P.C. Thüne, J. Laine, Cellulose nanocrystal submonolayers by spin coating, Langmuir 23 (19) (2007) 9674–9680.
[20] F. Li, H.-Y. Yu, Y.-Y. Wang, Y. Zhou, H. Zhang, J.-M. Yao, S.Y.H. Abdalkarim, K.C. Tam, Natural biodegradable poly (3-hydroxybutyrate-co-3-hydroxyvalerate) nanocomposites with multifunctional cellulose nanocrystals/graphene oxide hybrids for high-performance food packaging, J. Agric. Food Chem. 67 (39) (2019) 10954–10967.
[21] C. López de Dicastillo, L. Garrido, N. Alvarado, J. Romero, J. Palma, M. Galotto, Improvement of polylactide properties through cellulose nanocrystals embedded in poly (vinyl alcohol) electrospun nanofibers, Nanomaterials 7 (5) (2017) 106.
[22] T.C. Mokhena, J.S. Sefadi, E.R. Sadiku, M.J. John, M.J. Mochane, A. Mtibe, Thermoplastic processing of PLA/cellulose nanomaterials composites, Polymers 10 (12) (2018) 1363.
[23] M.F. Montemor, Smart Composite Coatings and Membranes: Transport, Structural, Environmental and Energy Applications, Elsevier, 2015.
[24] O. Moreno, L. Atarés, A. Chiralt, M.C. Cruz-Romero, J. Kerry, Starch-gelatin antimicrobial packaging materials to extend the shelf life of chicken breast fillets, LWT 97 (2018) 483–490.
[25] K. Müller, E. Bugnicourt, M. Latorre, M. Jorda, Y. Echegoyen Sanz, J. Lagaron, O. Miesbauer, A. Bianchin, S. Hankin, U. Bölz, Review on the processing and properties of polymer nanocomposites and nanocoatings and their applications in the packaging, automotive and solar energy fields, Nanomaterials 7 (4) (2017) 74.
[26] J.Y. Na, B. Kang, D.H. Sin, K. Cho, Y.D. Park, Understanding solidification of polythiophene thin films during spin-coating: effects of spin-coating time and processing additives, Sci. Rep. 5 (2015) 13288.
[27] T.B. Rouf, J.L. Kokini, Natural biopolymer-based nanocomposite films for packaging applications, Bionanocomposites for Packaging Applications, Springer 2018, pp. 149–177.
[28] M.D. Sanchez-Garcia, E. Gimenez, J.M. Lagarón, Morphology and barrier properties of solvent cast composites of thermoplastic biopolymers and purified cellulose fibers, Carbohydr. Polym. 71 (2) (2008) 235–244.
[29] S. Sangkasanya, P. Naknaen, N. Petchwattana, Feasibility application of biodegradable active films produced by poly (lactic acid) incorporating with limonene as an antimicrobial packaging for fresh beef meat, Proceedings of the 2018 8th International Conference on Bioscience, Biochemistry and Bioinformatics 2018, pp. 60–64.
[30] S. Shankar, L.-F. Wang, J.-W. Rhim, Incorporation of zinc oxide nanoparticles improved the mechanical, water vapor barrier, UV-light barrier, and antibacterial properties of PLA-based nanocomposite films, Mater. Sci. Eng. C 93 (2018) 289–298.
[31] A. Sharif, S. Mondal, M.E. Hoque, Polylactic acid (PLA)-based nanocomposites: processing and properties, Bio-based Polymers and Nanocomposites, Springer 2019, pp. 233–254.
[32] J. Shojaeiarani, D.S. Bajwa, N.M. Stark, Spin-coating: a new approach for improving dispersion of cellulose nanocrystals and mechanical properties of poly (lactic acid) composites, Carbohydr. Polym. 190 (2018) 139–147.
[33] L.T. Sin, B.S. Tueen, Polylactic Acid: A Practical Guide for the Processing, Manufacturing, and Applications of PLA, William Andrew, 2019.
[34] V. Siracusa, Food packaging permeability behaviour: a report, Int. J. Polym. Sci. 2012 (2012).
[35] Essential Oils Market Size, Share & Trends Analysis Report by Application (Cleaning & Home, Medical, Food & Beverages, Spa & Relaxation), by Product, by Sales Channel, and Segment Forecasts, 2019–2025, 2019 (Report ID, 978-1).
[36] N.M. Stark, L. Wei, R.C. Sabo, R.R. Reiner, L.M. Matuana, Effect of freeze-drying on the morphology of dried cellulose nanocrystals (CNCs) and tensile properties of poly (lactic) acid-CNC composites, Proceedings, ANTEC® 2018-Society of Plastics Engineers 2018, p. 5.
[37] J. Turner, A. Riga, A. O'Connor, J. Zhang, J. Collis, Characterization of drawn and undrawn poly-L-lactide films by differential scanning calorimetry, J. Therm. Anal. Calorim. 75 (1) (2004) 257–268.
[38] M.D. Tyona, A theoritical study on spin coating technique, Adv. Mater. Res. 2 (4) (2013) 195–208.
[39] D. Wang, W. Cheng, Q. Wang, J. Zang, Y. Zhang, G. Han, Preparation of electrospun chitosan/poly (ethylene oxide) composite nanofibers reinforced with cellulose nanocrystals: structure, morphology, and mechanical behavior, Compos. Sci. Technol. 182 (2019) 107774.
[40] C.J. Weber, Biobased Packaging Materials for the Food Industry: Status and Perspectives, a European Concerted Action, KVL, 2000.
[41] W. Yang, E. Fortunati, F. Dominici, G. Giovanale, A. Mazzaglia, G.M. Balestra, J.M. Kenny, D. Puglia, Synergic effect of cellulose and lignin nanostructures in PLA based systems for food antibacterial packaging, Eur. Polym. J. 79 (2016) 1–12.